# Influence of Skewing Design for Reduction of Force Ripples in DSL-SynRM using 3D FEA

Anusha Vadde, Sudha B

*Abstract*—**Double Sided Linear Synchronous Reluctance Motors (DSL-SynRM) are being increasingly used in high force density applications. The force ripples are one of the major issue in machine which is due to nonlinear nature of current in the machines. This paper focuses on the reduction of force ripples for increasing the force density of the motor. In order to reduce the force ripples, DSL-SynRM with a skewed translator is proposed. The proposed structure is designed and developed by using computational magnetic tools. This concept is effective for reduction of the force ripples and improves the force density of the machine. The proposed design has been reduced the percentage of force ripples by 21.62 %, improved the force density by 10.32 N/mm³ and efficiency by 0.89%.**

*Index Terms*— **DSL-SynRM, force density, force, force ripple, skewing, FEA**

## I. INTRODUCTION

A MASSIVE demand for linear motion technology offers wide applications in modern life. Commonly used linear electric motors for linear applications are Linear Switched Reluctance Motor (LRM) and Linear Synchronous Reluctance Motor (LSynRM). LSynRMs are used in applications like vertical train transportation and industrial sectors due to its high speed operation with multi flux barrier structure [1].

The linear synchronous reluctance motor works on the magnetic reluctance torque principle, in this maximum torque is produced due to difference between the aligned and unaligned position of a translator. LSynRM have stator and translator. The structure of LSynRM consists of axially slotted translator [2].Translator does not have any field winding. The stator has three phase symmetrical winding which creates sinusoidal rotating magnetic field in the air gap and the reluctance torque is developed. The stator of the motor is supplied with a supply. When the motor starts running 75% of synchronous speed, then the starting switch is disconnected from the motor. Motor gets accelerated and running close to synchronous speed at sufficient reluctance torque. The rotor of the motor aligns itself for low reluctance path. The induced magnetic field in the stator has a tendency to cause the translator to align with the stator field at a minimum reluctance position. At low reluctance, the rotor attains the synchronism and it remains at synchronism position due to synchronous reluctance torque. Torque angle is adjusted with respect to variation of load on the motor. The linear synchronous reluctance machines used in many applications like contactless train, vertical transportation, rope less elevator, servo drive, transportation sector, machine tool drives etc.

It has good starting torque and accurate speed control can be achieved. This motor is cost effective and easy maintenance. This motor has some disadvantages like noisy in operation, flux linkages, force ripples due to nonlinear function of stator currents and the position control of the rotor is challenge. These problems cause less efficiency and poor performance of the motor [3].

This problem can be reduced by various methods like modification of geometry, advance control strategy, Current profile, Force Distribution Force (FDF), and multi-phase excitation methods [4]. The single sided LSynRM is modified into Double Sided LSynRM (DSL-SynRM) to achieve position control of translator with respect to stator and also to reduce force ripples. The DSL-SynRM has either two stator and one translator (mover) or one stator and two translator vice versa [4]. Proposed DSL-SynRM in the present paper have two stator and one skewed translator. The windings are wound around the translator and excitation is given to translator for analysis purpose. In this paper, the skewed translator structure is proposed for DSL-SynRM to reduction of force ripples in the machine. The method of skewing and calculation of forces are analysed with analytically and numerically using Finite Element Analysis (FEA).

## II. DESIGN OF DOUBLE SIDED LINER SYNCHRONOUS RELUCTANCE MOTORS (DSL-SYNRMS)

### *A. Design of Double Sided Linear Synchronous Reluctance Motor (DSL-SynRM)*

A DSL-SynRM is designed based on the working principle of magnetic reluctance knowledge of single sided Linear SynRM [3]. The designing of a DSL-SynRM includes selecting the appropriate materials for stator and translator. Air gap flux density ($B_{avg}$) and specific electric loading ($A_{sp}$) are important factors for obtaining diameter of a DSL-SynRM. Winding factor ($K_w$), stacking factor ($k_i$), and end effect factor ($k_e$) are the determination of bore diameter for a DSL-SynRM [5-7]. DSL-SynRM stator has no winding and it has flux barriers. The better performance of the motor is obtained when the flux barriers are introduced. There are two different rotor flux paths. One is high permeability path that is the flux lines are flowing in the rotor iron paths, it is parallel to the flux barriers, and it is

Manuscript was submitted for review on 08, October, 2018.

Anusha vadde is working in M.S. Ramaiah University of applied sciences.(e-mail: vaddeanusha203@gmail.com).

Sudha B is working in Ramaiah University of applied sciences. (e-mail: sudha.ee.et@msruas.ac.in).

Digital Object Identifier 10.30941/CESTEMS.2019.00052

generally called as d-axis path. Second is low permeability path, in this - flux lines have to cross the rotor flux barriers. It is generally called as q-axis path.

The flux barriers can be introduced by using non ferromagnetic materials. Low reluctance in d-axis and high reluctance in q-axis is obtained by using flux barriers. In the paper rectangular shaped steel flux barriers are chosen to increase the flux path and it is shown in Fig. 1.

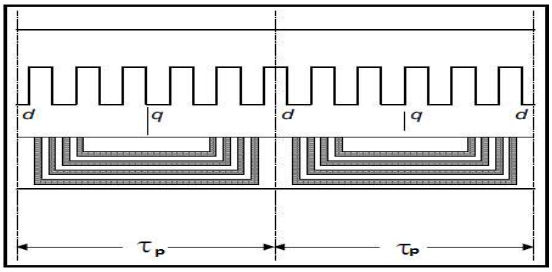


Fig. 1. Linear SynRM with Flux Barriers.

The design of flux barriers is important in LSynRM, proper design of flux barriers reduces the force ripples [5]-[8]. The design of stator should satisfy the conditions are as follows

- The main flux in d-axis has to flow across the whole pole surface in order to obtain maximum inductance ($L_d$).
- The flowing of flux should be minimum in q-axis, because to get low value of magnetising inductance ($L_q$).

The voltage balances in d and q axes are described as

$$\begin{bmatrix} V_d \\ V_q \end{bmatrix} = R \begin{bmatrix} i_d \\ i_q \end{bmatrix} + \frac{d}{d_t} \begin{bmatrix} \psi_d \\ \psi_q \end{bmatrix} + \frac{\pi}{\tau_p} \frac{d_x}{d_t} \begin{bmatrix} -\psi_q \\ \psi_d \end{bmatrix} \quad (1)$$

Where

$\psi_d$ = Flux linkages in'd' axis
$\psi_q$ = Flux linkages in 'q' axis
$i_d$ = Current in'd' axis winding
$i_q$ = Current in 'q' axis winding
$V_d$ = Voltage across 'd' axis winding
$V_q$ = Voltage across 'q' axis winding

### *B. Design of Flux Barriers*

The designing of flux barriers and placement of flux barrier or air barrier is depends on the q-axis and d-axis. The flux barrier does not affect the d-axis flux distribution and it blocks the q-axis flux distribution [5]-[9].

### *C. Design of Translator*

The translator of a DSL-SynRM includes winding and it is active part of the DSL-SynRM. According to the value of pole pitch ($\tau_p$), the number translator slots ($N_{ts}$) are decided as 16 slots and number of pole (P) is 4.

### *D. Selection of Pitch ($\tau_p$)*

The selection of pole pitch for a DSL-SynRM is mainly depends on the magnetic reluctance principle. Here, the pole pitch is defined as a peripheral distance between center of two adjacent segments of stator. This distance is measured in terms of translator slots between two adjacent segments of stator centers. The selection of pole pitch values varies 40 mm < $\tau_p$ < 70 mm and it depends on the conductors in the translator winding [10]-[12].

Finally, arrived schematic view of a DSL-SynRM is shown in Fig. 2, it consists of 4 poles with 3 flux barriers on stator and 18 slots with concentric winding on translator. The total lengths, width and height of the DSL-SynRM are included in dimensional specifications and they are tabulated in Table .I. In this paper, skewed translator structure is introduced for reduction of fringing flux and force ripples. The efficiency and power factor of DSL-SynRM is improved and force ripples are reduced by adopting the skewing structure design in motor.

TABLE I
SPECIFICATIONS OF THE DSL-SYNRM

| Variable | Values |
|---|---|
| Velocity ($V_m$) | 2.5 m/s |
| Acceleration ($a_a$) | 3.35 m/s$^2$ |
| Power capacity (P) | 162.5 watts |
| Input current ($I_a$) | 10 A |
| Number of slots ($N_{ts}$) | 18 |
| Translator Pole(secondary) ($N_t$) | 4 |
| Stator Pole(primary) | 4 |
| Pole Pitch ($T_p$) | 60mm |
| Number of Flux Barriers (k) | 3 |
| Winding Factor ($k_w$) | 0.9 |
| Air gap | 1mm |
| Steel Type | M19_24G |
| Barriers Width ($R_b$) | 1mm |
| Total width of the designed DSL-SynRM | 240mm |
| Total height of the designed DSL-SynRM | 154mm |

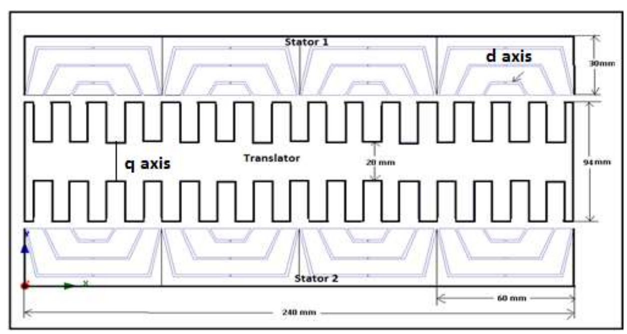


Fig. 2. Schematic View of Designed DSL-SynRM.

The motor thrust force or average force is,

$$F_e = \frac{\pi}{\tau_p} \left( \psi_d i_q - \psi_q i_d \right) \quad (2)$$

The force on both the axes is obtained with flux distribution and current in particular axis. The inductance for x axis is calculated by [13-14],

$$L(i_p, x) = \sum_k L_k(i_p, x) = \frac{T_{ph}}{i_p} \cdot \sum_k \emptyset_k(i_p, x) \quad (3)$$

where

$L(i_p, x)$ = Inductance value at x axis with its peak current,
$L_k(i_p, x)$ = Inductance value at k$^{th}$ path in x axis
$\emptyset_k(i_p, x)$ = Magnetic flux at k$^{th}$ path in x axis

## III. MODEL OF DSL-SYNRM WITHOUT SKEWING STRUCTURE

The design of a DSL-SynRM without skewing structure has been implemented using ANSOFT Maxwell computational tool. In this motor, pole pitch plays an important role for winding the stator with respect to translator.

The basic 3D structure of DSL-SynRM is shown in Fig. 3, it has 18 slots of translator and four pole pitches on one side of the stator, so that each pole pitch consists of three flux barriers. The three air gap flux barriers are placed for reduction of magnetic saturation, slotting effect. The translator part consists of 3 phase winding which is placed over on slots. The M19_24G steel material is assigned to both stator and translators of a DSL-SynRM for strong magnetic flux distribution. The inside length based meshing is assigned to the stator, translator and coils of the DSL-SynRM. The Dirichlet boundary condition is assigned for periphery of the geometry, for analyzing of force, inductances and flux linkages. The model of DSL-SynRM without skewing structure is shown in Fig. 3. It has two stators (passive) and one translator (active) structure.

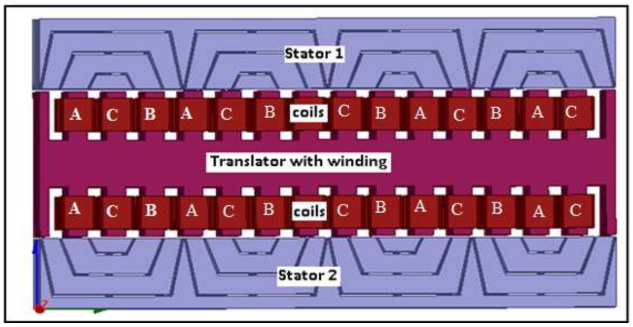


Fig. 3. 3D Model of DSL-SynRM without Skewing Structure.

The magnetic flux distribution in DSL-SynRM without skewing structure for unaligned and aligned positions are analyzed for sinusoidal excitation current of 10 A. The propulsion force, inductance and flux linkages are analyzed for unaligned position to the aligned position over a two pole pitch. The magnetic flux distribution in DSL-SynRM without skewing structure for unaligned position is as in Fig. 4. A rated current of 10 A has been given to switching phase A, B and C respectively as shown in Fig. 3. Therefore, north and south poles are formed based on Fleming's right hand thumb rule and the mutual flux is observed at another switching phases. From Fig. 4, each pole pitch is moved from 30 mm distance to complete cycle of magnetic flux path with respect to the translator position.

The magnetic flux lines are distributed radial through the flux barriers of stator to translator poles. The force developed by the translator is zero due to unaligned position of translator. The magnetic flux distribution in DSL-SynRM without skewing structure for aligned position is as shown in Fig. 5. A rated current of 10 A is given to switching phase A, B and C respectively so that magnetic flux is distributed through the all poles of translator. Here, pole pitch is considered from origin to complete cycle of flux path with respect to the translator position. The magnetic flux lines are distributed radial through the flux barriers of stator to translator poles are shown in Fig. 5. In this case, leakage flux is high in air-gap between flux barriers to the translator poles, increases the fringing flux. The force developed by the translator is zero due to unaligned position of translator.

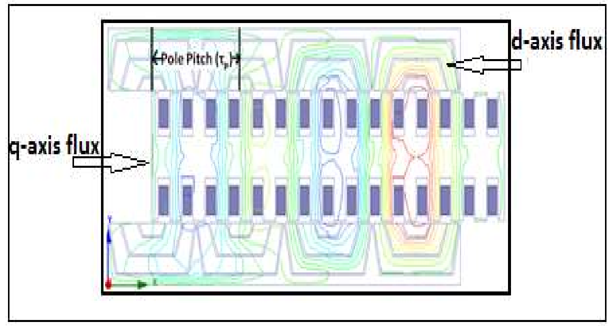


Fig. 4. Magnetic Flux Distribution in Unaligned Position.

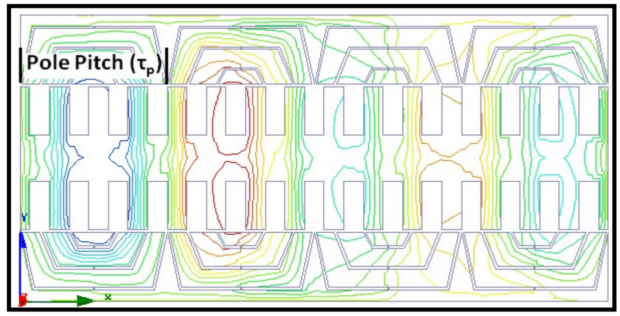


Fig. 5. Magnetic Flux Distribution in Aligned Position.

## IV. Analysis of Force Ripples in DSL-SynRM

Switching the two consecutive phases of the DSL-SynRM leads to the force ripples in the machine. The propulsion force has developed by the translator position of DSL-SynRM is shown in Fig. 6. The maximum and minimum forces are $F_{max}$ and $F_{min}$. These two forces occurs at the intersection point of two consecutive phases [14-16]. The percentage of force ripples are calculated by,

$$\%F_{ripple} = \frac{(F_{max} - F_{min})}{F_{avg}} \times 100 \qquad (4)$$

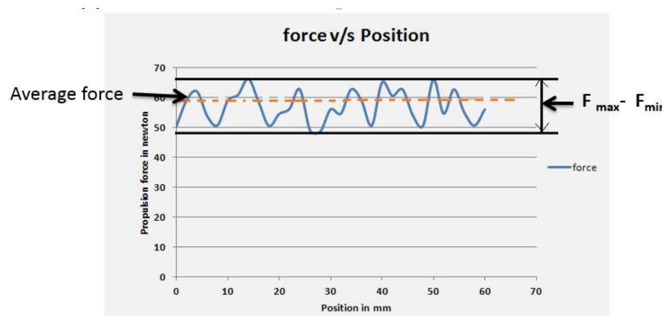


Fig. 6. Propulsion Force with respect to Translator Position.

## V. Analysis of Skewing Concept in DSL-SynRM

The skewed structure of a DSL-SynRM as in Fig. 7, the skewing of the pole width ($b_s$) helps to reduce fringing flux between stator and translator pole of a DSL-SynRM. The pole area ABCD and after skewing of a DSL-SynRM pole area becomes ADEB as shown in Fig. 7. Generally normal force and propulsion forces are acting on the pole area along 'y' and 'x' axes. Distribution of normal force along the line 'AC' and 'AD' and propulsion force acting on 'AB' and 'DE' are different for vertical and skewed structures respectively. From the Fig. 7, the skewing angle can be derived as

$$\tan\theta = \left(\frac{\text{slot width}(b_s)}{L_w}\right) \quad (5)$$

$$\theta_{skew} = \tan^{-1}\left(\frac{slot\ width(b_s)}{L_w}\right) \quad (6)$$

Where, $L_w$ is the stack length of a DSL-SynRM and $b_s$ is the slot width. As refer to "(6)" skewing angle ($\theta_{skew}$) varies from $0^0 < \theta_{skew} < 90^0$, it cannot go above these values.

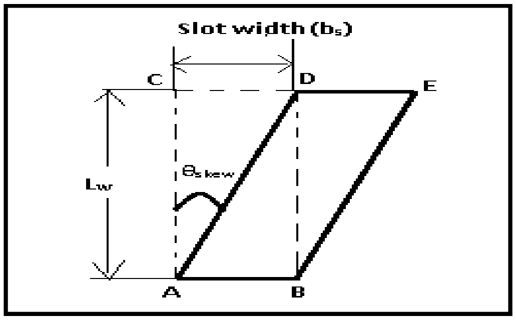


Fig. 7. Skewing Concept in DSL-SynRM.

Let, $L_w$ = 50 mm and $b_s$= 8 mm then the skewing angle is calculated as

$$\theta_{skew} = \tan^{-1}\left(\frac{\text{slot width}(b_s)}{L_w}\right) = \tan^{-1}\left(\frac{8}{50}\right) = 9^0 \quad (7)$$

Therefore, finally skewing angle $\theta_{skew}$ varies for design is from $0^0 < \theta_{skew} \leq 9^0$.

## VI. Model of DSL-SynRM with Skewing Structure

3D Model of a DSL-SynRM with skewing structure is shown in Fig. 8. The basic principle involved in it is similar to the DSL-SynRM without skewing structure. The translator of the DSL-SynRM has skewed using "(7)". The DSL-SynRM with skewing structure consists of four Pole Pitches on each side of the stator and translator with 18 slots.

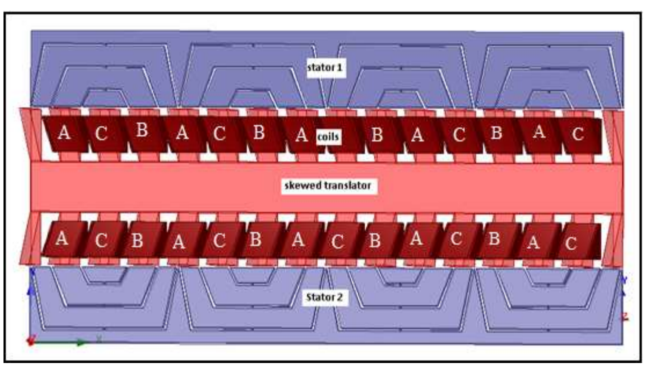


Fig.8. Designed 3D Model of a DSL-SynRM with Skewing Translator Structure.

Magnetic flux distribution has been analyzed for the proposed model at different positions of the translator. Translator is moving from unaligned position to aligned position for the given constant excitation current of 10 A. The propulsion force, inductance and flux linkages are observed at each translator positions. In this case, magnetic flux distribution for unaligned position is similar to the magnetic flux distribution in DSL-SynRM without skewed structure.

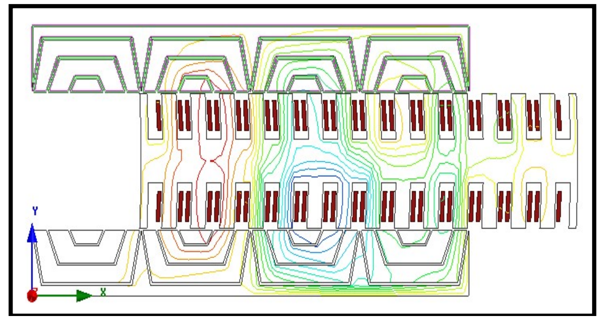


Fig. 9. Mangetic Flux Distribution in Aligned Position.

The magnetic flux distribution in DSL-SynRM with skewing structure for aligned position is as shown in Fig. 9. A rated current of 10 A has been given to switching phase A, B and C respectively so that magnetic flux is distributed through the all poles of translator. In this case, leakage flux is less in air-gap between flux barriers to the translator poles, reduces the percentage of fringing flux.

## VII. Results

### A. *DSL-SynRM without Skewing*

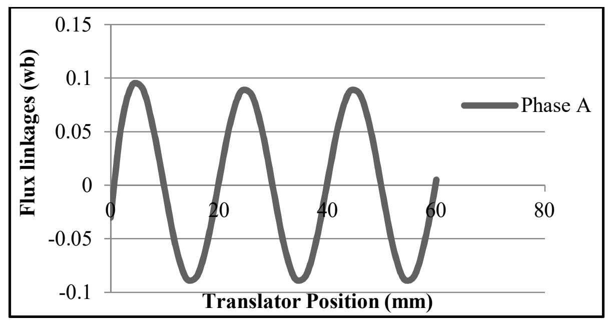


Fig. 10. Flux Linkage with Respect to Translator Position.

The obtained flux linkage from FEA results is 0.1 wb is observed in Fig. 10. The obtained plot is in sinusoidal in nature because of sinusoidal excitation is applied to the coils. The flux linkages are theoretically calculated using "(8)" and verified with FEA results.

$$B_k = \frac{\emptyset_k(i_p, x)}{A_k} \quad (8)$$

Where, $A_k$ = Cross- section area in path k

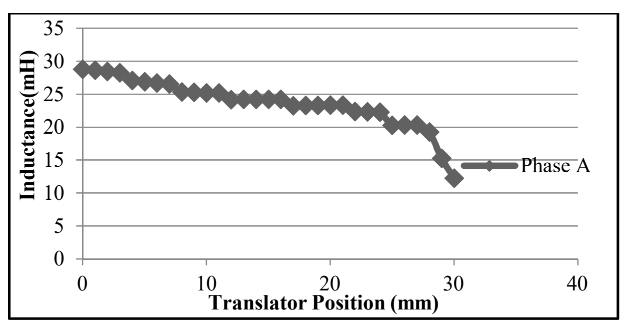


Fig. 11. Inductance with Respect to Translator Position

Fig. 11 represents the inductance with respect to translator for given sinusoidal excitation of phase 'A'. From Fig. 11, at 0 mm indicates aligned and at 30 mm unaligned inductances are captured. The variations of inductance are gradually decreasing from maximum to minimum. From the plot, aligned inductance ($L_d$) is 23.56 mH and unaligned inductance ($L_q$) is 12.3 mH.

The inductances are verified theoretically using “(3)”. The inductance is maximum for aligned position and minimum for unaligned position due to reluctance principle.

### *B. DSL-SynRM with Skewing*

The plots of propulsion force, inductance and flux linkages with respect to translator position are similar for all excitations. The switching phases are excited with a rated current of 10 A at optimized skewing angle of $9^0$. The plot of flux linkages with respect to translator for given sinusoidal excitation of phase ‘A’ is shown in Fig. 12. From Fig. 12, at 0 and 60 mm indicates the unaligned and aligned positions. The flux linkages is sinusoidal in nature due to given excitation is in sinusoidal. The plot of the value of flux linkages is 0.09 wb and is verified theoretically using “(8)”.

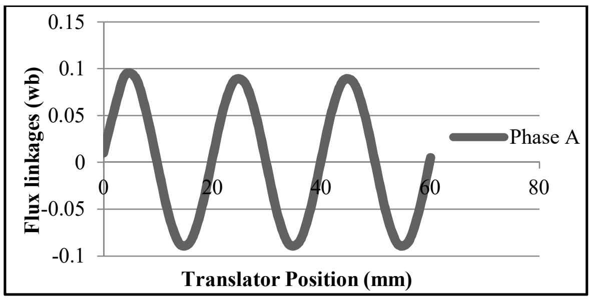


Fig. 12. Flux Linkage with Respect to Translator Position.

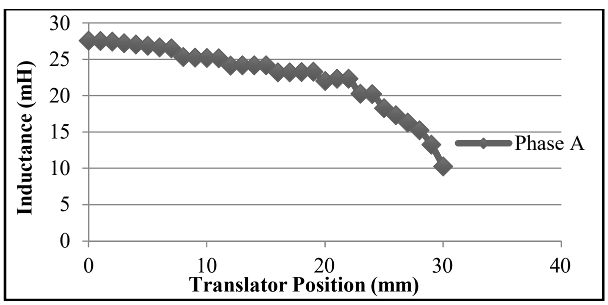


Fig. 13. Inductance with Respect to Translator Position.

Fig. 13 represents the plot of inductance with respect to translator for given sinusoidal excitation of phase ‘A’. From Fig. 13, at 0 mm indicates aligned and 30 mm indicates unaligned positions. By observing the plot, the aligned inductance is 23.8 mH and the unaligned inductance is 10.2 mH. The inductance values are improved in skewing structure using “(3)”.

## VIII. VALIDATION OF RESULTS FOR DSL-SYNRM WITH AND WITHOUT SKEWED STRUCTURE

The inductance of a DSL-SynRM with and without skewing structure for different translator positions are calculated using “(3)” and the obtained values of aligned inductance ($L_d$) and unaligned inductance ($L_q$) are tabulated in Table II.

TABLE II
COMPARISION OF INDUCTANCE VALUES

| Inductance(L) | Analytical | FEA(Without Skewing) | FEA(With Skewing) |
|---|---|---|---|
| Aligned ($L_d$) | 23.6 mH | 23.56 mH | 23.8 mH |
| Unaligned ($L_q$) | 11.7 mH | 12.3 mH | 10.2 mH |

The force ripples for without and with skewed design are computed using “(4)” and are tabulated in TABLE III. It clears that $9^0$ skewing of translator gives force of 63.5 N and force ripple reduced to 20% than without skewing design.

The total loss is,

$$P_{loss} = P_{iron} + P_{cu} \tag{9}$$

TABLE III
COMPARISION OF AVERAGE FORCE VALUES

| Skewing angle | $F_{max}$ (N) | $F_{min}$ (N) | $F_{avg}$ (N) | % Force Ripple |
|---|---|---|---|---|
| Existing($0^0$) | 135.82 | 104.67 | 60.05 | 51.8 |
| $3^0$ | 112.65 | 88.7 | 62.15 | 38.15 |
| $4^0$ | 115.26 | 89.6 | 61.9 | 41.45 |
| $5^0$ | 116.7 | 88.96 | 60.02 | 46.07 |
| $6^0$ | 117.01 | 90.7 | 61.5 | 44.4 |
| $7^0$ | 119.5 | 92.5 | 62.01 | 43.47 |
| $8^0$ | 120.7 | 98.64 | 62.5 | 35.6 |
| $9^0$ | 122.6 | 103.4 | 63.5 | 30.18 |

TABLE IV
COMPARISION OF EFFICIENCY FOR DSL-SYNRM

| Parameter | Without Skewed Structure DSL-SynRM | With Skewed Structure DSL-SynRM |
|---|---|---|
| Efficiency | 75.15% | 76.04% |
| Ripple | 51.80% | 30.18% |
| Power factor(PF) | 0.39 | 0.42 |
| $P_{cu}$ | 39.4 W | 38.4 W |
| $P_{iron}$ | 10.5 W | 9.7 W |

Efficiency is computed using equation

$$\text{efficiency } (\eta)=\frac{P_{out}}{P_{out}+P_{loss}}\times 100 \tag{10}$$

The efficiency of the existing DSL-SynRM is calculated by

$$\text{efficiency}(\eta) = \frac{150}{150 + 40.9} \times 100 = 75.15\%$$

Similarly efficiency for DSL-SynRM with skewed structure is calculated as

$$\text{efficiency}(\eta)=\frac{158.75}{158.75+40.9}=76.04\%$$

The power factor for DSL-SynRM is obtained by

$$PF = \left[\frac{L_d-L_q}{L_d+L_q}\right] \tag{11}$$

Efficiency and force ripple for without and with skewed design are tabulated in TABLE IV. It clears that the proposed design efficiency is increased to 0.89% and force ripples are reduced to 20% in DSL-SynRM.

### *A. Force Density*

The force density of the DSL-SynRM without and with skewing structure can be calculated with the ratio of average propulsion force to the volume of the stator ($V_{stator}$) of the DSL-SRM is calculated using equation

$$\text{Force Density} = \frac{F_{avg}}{V_{stator}}\times 9.81 \tag{12}$$

The volume of the stator ($V_{stator}$) is calculated by

$$V_{stator} = 4.m.\alpha_p\beta_p T_s^2 L_w \tag{13}$$

here $\alpha_p$ and $\beta_p$ is given by

$$\alpha_p = \frac{b_s}{T_s} = 0.2$$

$$\beta_p = \frac{h_s}{T_s} = 0.925$$

From "(13)", $V_{stator} = 2.95 \times 10^{-3}$ m$^3$ and force density is 211.49 N/mm$^3$ is obtained.

TABLE V
COMPARISION OF FORCE DENSITY BETWEEN WITHOUT SKEWED AND WITH SKEWED PROPOSED DESIGN OF A DSL-SYNRM

| Force density | Without skewed design (N/mm$^3$) | With skewed design (N/mm$^3$) |
|---|---|---|
| DSL-SynRM | 201.18 | 211.49 |

### *B. Selection of the Skew Angle and Advantages*

The selection of skew angle is considered for the following reasons

- The structure of the rotor for the given specifications has been intersected to the stator design of flux barriers for beyond the angle of $9^0$
- The normal force on the motor along 'y' axis decreases as above the considered skew angle. It leads to stress on the pole area and causes deformation of the translator.

Advantages are as follows

- Total motor mass and volume of the rotor is reduced compared to the skewed structure
- The temperature of the motor is decreases since iron and copper losses are reduced in skewed translator of motor as compared to the conventional structure
- Force density of the motor is improved with the reduced mass and same specifications of the motor

## IX. CONCLUSION

The proposed 4 pole, 18 slots, 12 V DSL-SynRM with without skewed structure has been implemented in ANSOFT Maxwell tool. The optimized skewing of translator has been designed as $9^0$. The proposed DSL-SynRM with skewed structure reduces the force ripples by 21.62%, force density and efficiency improved by 10.32 N/mm$^3$ and 0.89%. Force ripples for DSL-SynRM can be reduced by adding control strategies to the optimized geometry. Power factor for DSL-SynRM can be improved by increasing the saliency ratio. Multi-phase excitation using appropriate control strategies can be suggested for DSL-SynRM for reduction of ripples.

## REFERENCES

[1] Sanada, M., Asano, M., Morimoto, S., & Takeda, Y. (2000). Mover Design and Performance Analysis of Linear Synchronous Reluctance Motor with Multi-flux Barrier. *IEEJ Transactions on Industry Application*. [Online]. *120(7),* pp. 922-927. Available: https://www.jstage.jst.go.jp/article/ieejias1987/120/7/120_7_922/_pdf

[2] Jacek F. Gieras, "Linear Synchronous Motors-Transportation and Automation Systems", 2nd ed., New York: Taylor and Francis, 2012.

[3] *Avinash Konkani,* Rabindranath Bera, Samrat Paul, "Advances in Systems, Control and Automation", Springer, 2016.

[4] N. Bianchi, The Rediscovery of Synchronous Reluctance and Finite Permanent Magnet Motors, Tutorial Course Notes, Springer Briefs in Electrical and Computer Engineering, 2016.

[5] Stumberger, G., Stumberger, B., & Dolinar, D.. Identification of linear synchronous reluctance motor parameters. *IEEE transactions on industry applications,* vol. 40, no. 5, pp. 1317-1324, 2004.

[6] Moghaddam, R.R., *Synchronous Reluctance Machine (SynRM) Design,* Master Thesis, Dept. of Electrical Engineering, Royal Institute of Technology, Stockholm, 2007.

[7] Dirba, J., Lavrinovicha, L., & Dobriyan, R.. Study of the synchronous reluctance motor design. *Latvian Journal of Physics and Technical Sciences*. vol. 53, no. 4, pp. 22-29, 2016.

[8] Rick. S, Putri A.K., Franck. D, Hameyer. K, "Permanent magnet synchronous reluctance machine—Design guidelines to improve the acoustic behaviour", In *Proc. of International Conference Electrical Machines (ICEM),* 2014, pp. 1383-1389.

[9] Moradi Cheshmehbeigi, H., & Fathinia, F.. The finite element analysis of the linear hybrid reluctance motor for the electromagnetic launch system. *Energy Equipment and Systems*. vol. 5, no. 4, pp. 401-409, 2017.

[10] Lenin, N. C., & Arumugam, R.. Design and experimental verification of linear switched reluctance motor with skewed poles. *International Journal of Power Electronics and Drive Systems*. vol. 6, no. 1, pp. 18, 2015.

[11] Mahmoud, H., & Bianchi, N.. Eccentricity in synchronous reluctance motors—Part II: Different rotor geometry and stator windings. *IEEE Transactions on Energy Conversion*. vol. 30, no. 2, pp. 754-760, 2015.

[12] Štumberger, G., Štumberger, B., Dolinar, D., Težak, O., & Hameyer, K. Nonlinear model of linear synchronous reluctance motor for real time applications. *COMPEL-The international journal for computation and mathematics in electrical and electronic engineering*. vol. 23, no. 1, 316-327, 2004.

[13] Pehrman, D, Jones, M., "Start capability of industrial synchronous motor with high efficiency reduction of double-sided linear switched reluctance motor", In *Proc. of 11th International Symposium on LDIA,* 2017, pp. 1-5.

[14] Lubin, T, Hamiti, T, Razik, H. and Rezzoug, A.. Comparison between finite-element analysis and winding function theory for inductances and torque calculation of a synchronous reluctance machine*, IEEE Transactions on Magnetics*. vol. *43, no.* 8, pp. 3406-3410, 2007.

[15] Dolinar, D., Stumberger, G., Zagradisnik, I., & Hameyer, K., "Exact tracking of linear synchronous reluctance servo drive". *In Proc. of ICEM,* 2000, vol. 1, pp. 94-98.

[16] Bae, H. K., Lee, B. S., Vijayraghavan, P., & Krishnan, R.. A linear switched reluctance motor: converter and control. *IEEE Transactions on Industry Applications*. vol. *36, no. 5,* pp. 1351-1359, 2000.

**Anusha vadde** was born in Andhra Pradesh, India, 1990. She Graduated from JNTU Kakinada University in 2011 and the M.Sc [Engg.] degree from Coventry University in 2014. She got young innovation award from Rastrapathi Bhavan. She is working in M.S. Ramaiah University of applied sciences from 2014 to till now. She has been working toward the Ph.D. degree at Ramaiah University of applied sciences. Her current research interests are FEM analysis of electrical machines.

**Sudha B.** was born in Karnataka, India, 1991**,** She Graduated from Visvesvaraya Technological University, belgaum in 2013 and the M. Tech. degree from Ramaiah university of applied science in 2017. She is working in Ramaiah University of applied sciences from 2017 to till now. She has been working toward the Ph.D. degree at Ramaiah University of applied sciences. Her current research interests are electromagnetic and thermal analysis of induction electrical machines.